Radiative and Nonradiative Transitions in $LaCl_3$: Pr and $PrCl_3$

K. R. German and A. Kiel
Bell Telephone Laboratories, Holmdel, New Jersey 07733
(Received 9 May 1973)

We have measured the fluorescent decay rates of the $^3P_0$ and $^3P_1$ states of the Pr^{3+} ion in $PrCl_3$ and $LaCl_3$ over a wide range of temperatures. At low temperatures the radiative lifetime of the $^3P_0$ state in $LaCl_3$:1-at.% Pr is 14.7 ± 1 μsec, while at room temperature in $PrCl_3$ the nonradiative lifetime is ≈ 0.38 μsec. In the dilute crystal the three-phonon-relaxation lifetime of the $^3P_1 \rightarrow {}^3P_0$ decay has been determined to be 3.1 ± 0.3 μsec. We have also set a new much lower limit on the nonradiative-decay lifetimes of the $^3P_2$ and $^1I_6$ states of $\tau \leq 1.5$ nsec. Some major discrepancies between our results and previous work are noted and, in several cases, resolved. A more refined model of the relaxation processes in the ^3P states is described which qualitatively explains the exceptionally large relaxation rates of the $^3P_2$ state and the much slower $^3P_1$ decay rate. We demonstrate that the detailed excited-state composition must be considered to explain the relative magnitudes of relaxation rates.

I. INTRODUCTION

The recent development of pulsed tunable dye lasers spanning the entire visible spectrum[1] now allows the selective excitation of many energy levels in paramagnetic crystals. The spectral intensity and time resolution available with this new excitation method far exceed that attainable with previous flash-lamp-pumping techniques. A number of problems involving nonradiative interactions in paramagnetic crystals may now be amenable to detailed study. In particular, there has been considerable recent interest in the fluorescent properties of concentrated rare-earth materials since it has been demonstrated that these crystals could, after all, display stimulated emission.[2-5] The radiative- and nonradiative-decay mechanisms have a crucial bearing on the properties of laser transitions. In the course of our study[4] of stimulated emission in $PrCl_3$, we observed significantly different decay rates than those reported in the literature.[6-8] This led us to make a detailed investigation of the decay processes in $PrCl_3$ and the dilute analogue $LaCl_3$: Pr.

The energy-level system of the trivalent-rare-earth crystals $PrCl_3$ and $LaCl_3$: Pr are among the simplest and best understood of any paramagnetic crystals. A partial energy-level diagram of Pr^{3+} (f^2 configuration) is shown in Fig. 1. A substantial number of sharp fluorescent transitions makes Pr^{+++} nearly ideal for the study of optical-transition lifetimes and nonradiative-decay phenomena. We have pumped these crystals in the regions of the $^3P_0$, $^3P_1$, $^1I_6$, and $^3P_2$ states. We were able to resolve some of the discrepancies with earlier work by careful analysis of all decay paths and have also set new, much smaller upper limits on the nonradiative-decay time for the $^3P_2$, $^1I_6 \rightarrow {}^3P_1$ nonradiative decays.

In Sec. II we describe the experimental technique used in these experiments. Sections III A and III B contain experimental results for the dilute and concentrated material, respectively, when pumping $^3P_0$ and $^3P_1$. Section III C is an analysis of those results in terms of rate equations. In Sec. IV we discuss nonradiative decay by multiphonon relaxation and its application to $^3P_1$-decay processes. We propose a new path for the $^3P_2 \rightarrow {}^3P_1$ decay in Sec. IV.

II. EXPERIMENT

The crystals used were fairly small (~10×4×2 mm) cleaved samples of either $PrCl_3$ or $La_{0.99}Pr_{0.01}Cl_3$ grown by Guggenheim. The crystals were mounted in quartz cuvettes under a helium atmosphere and sealed with rubber cement to retard surface deterioration by water vapor. Adequate surface quality could be maintained for several low-temperature runs by this simple method.

The cuvettes were mounted in a small glass Dewar into which cold nitrogen or helium gas was blown. The temperature was determined with either a thermocouple or calibrated carbon resistance thermometer.

The crystals were optically excited with a nitrogen-laser-pumped dye laser which had a peak power of 11 kW, a spectral width of 6 GHz, and a pulse width of 4 nsec (full width at half-maximum). The repetition rate could be varied from 1 to 100 Hz.

The crystal fluorescence was dispersed by a Jarrell-Ash 1-m spectrometer (limiting resolution ~0.06 Å in first order) and detected by a photomultiplier (EMI 9558A) with S-20 response. The output of the phototube was either averaged by a boxcar integrator or directly displayed on an oscilloscope. For qualitative measurements, the scope display was photographed; however, for accurate measurements, the boxcar gate was swept over a time interval corresponding to a change of about a factor of 10 in the fluorescent intensity (~2.4 decay

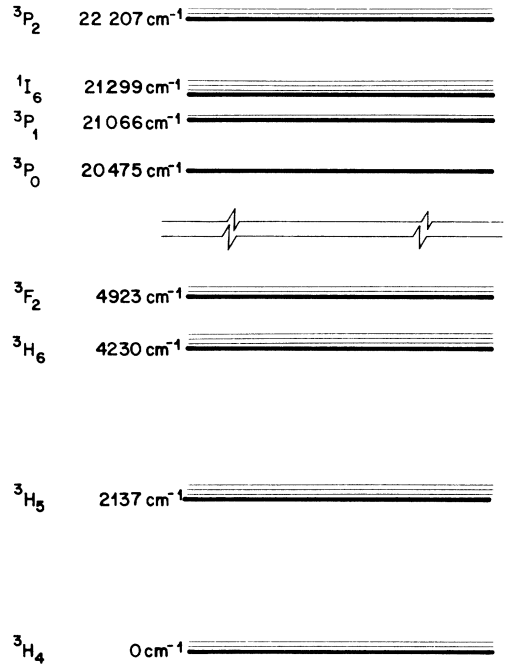

FIG. 1. Partial energy-level diagram of $LaCl_3$: Pr. The splitting within J manifolds are purely illustrative. The $^3F_3$ (6280-cm^{-1}), $^3F_4$ (6700 cm^{-1}), $^1G_4$ (9733-cm^{-1}), $^1D_2$ (16 630-cm^{-1}), and $^1S_0$ (48 800-cm^{-1}) manifolds have been omitted.

time constants). The intensity versus time data were fit to a single-exponential decay curve. The ultimate time resolution of the system was limited by the speed of the photomultiplier to about 20 nsec. Since the shortest decay time measured with this system was about 400 nsec, the photomultiplier response was not a serious limitation.

III. EXPERIMENTAL RESULTS

A. $LaCl_3$: 1-at.% Pr

The fluorescent lifetime of the $^3P_0$ state in dilute $LaCl_3$: Pr has been studied by Barasch and Dieke[6] using optical excitation and by Low *et al.*[7] with x-ray excitation. Dorman[8] has indirectly measured the radiative lifetime by determination of oscillator strengths in absorption. The three measurements are in reasonable agreement; Barasch and Dieke quote 13 μsec for the $^3P_0$ compared to the Low *et al.* value of 15 ± 2 μsec and the Dorman determination of 18.4 μsec.

In Fig. 2, our measurement of the total fluorescent decay time[9] of $^3P_0$ is plotted as a function of temperature for both the dilute sample and pure $PrCl_3$.[10] In each case, there is a monotonic decrease in the decay rate as the temperature decreases.[11] This is consistent with the total decay rate being the sum of a radiative decay rate which is independent of temperature and a temperature-dependent nonradiative-decay rate. The nonradiative component decreases with decreasing temperature but the exact functional dependence depends on the details of the nonradiative decay. Although the nonradiative rate does not go to zero at 0 K, we argue that for the dilute crystal it is small enough to be considered negligible compared to the radiative decay. This follows from the fact that $^3P_0$ is about 4000 cm^{-1} above the $^1D_2$ state which corresponds to the energy equivalent of about 18 optical phonons and, moreover, is spin forbidden. Experience with nonradiative decays in dilute rare-earth crystals indicates that such a nonradiative process should be negligible at low temperatures.[12–14] (We shall discuss this further in Sec. IV.) We therefore claim that the extrapolated value for the lifetime of the dilute crystal in Fig. 2, 14.7 ± 1.0 μsec is the real radiative-decay lifetime of the $^3P_0$ state. This is reasonably close to the values quoted above from previous work. The "gentle" variation of the decay time, from ~13 μsec at room temperature to 14.7 μsec at low temperatures, shows that the nonradiative-decay time at room temperature cannot be less than ~110 μsec. However, the 10% increase in lifetime at low temperature could be simply due to a change in the radiative transition rates because of thermal variation in the lattice crystal field. In that case the nonradiative lifetime at room temperature could be much longer

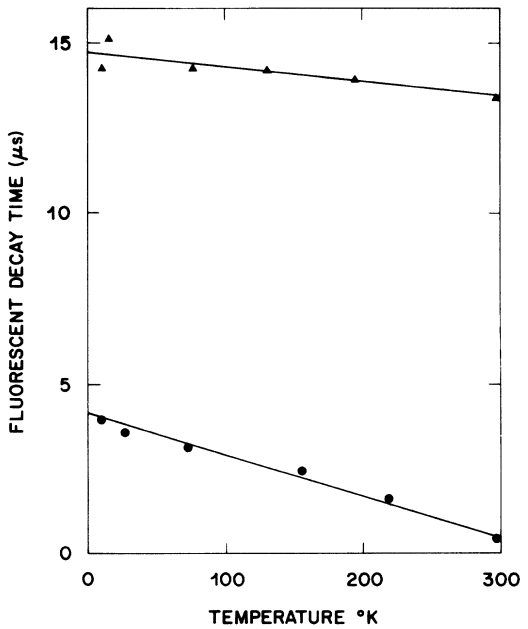

FIG. 2. Decay time of $LaCl_3$: Pr (triangles) and $PrCl_3$ (dots) plotted as a function of temperature. The relative change with temperature is much greater in $PrCl_3$ than in the dilute crystal.

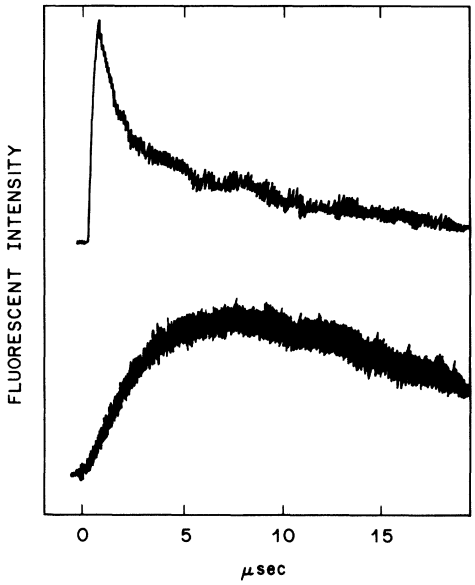

FIG. 3. Oscilloscope photographs of fluorescent intensity vs time for $^3P_1$ and $^3P_0$ states on pumping $^3P_1$; (a) $^3P_1$ emission, (b) $^3P_0$ emission.

than 110 μsec.

When the $^3P_1$ state is selectively excited, we observe fluorescence from both the $^3P_1$ state ($\lambda = 530$ nm, $^3P_1 \rightarrow {}^3H_5$ transition) and the $^3P_0$ state at all temperatures. This is as one would expect so long as the radiative-decay rate of $^3P_1$ and nonradiative-decay rate to $^3P_0$ are "comparable." A plot of the decay rate of the $^3P_1$ fluorescence versus temperature surprised us when the decay rate appeared to increase as the temperature was reduced below 300 K. In addition, the plots of the logarithm of intensity versus time were curved indicating that the decay curves were not of single exponential character. At 300 K, the decay rate of $^3P_1$ was nearly identical to that of $^3P_0$ at the same temperature (13.2 μsec). Oscilloscope photographs showing the double decay rates for $^3P_1$ and the slow buildup of $^3P_0$ are presented in Fig. 3. The complex decay curve was previously observed by Low *et al.*[7] who report a double decay of 4.5 and 14 μsec at 300 K. Barasch and Dieke report a decay time of 5 μsec for $^3P_1$ at 4 K while Dorman's measurements would imply a radiative lifetime of 37 μsec at low temperatures. The source of these anomalies became clear when we observed that when pumping the $^3P_0$ state at room temperature, we obtained strong fluorescence from $^3P_1$ despite the fact that it lies 591 cm^{-1} above $^3P_0$. The complex decay curves and anomalous temperature dependence are clearly due to the nonradiative transfer $^3P_1 \rightarrow {}^3P_0 \rightarrow {}^3P_1 \cdots$. A detailed discussion of this process will be postponed to Sec. III C. The variation with temperature of the intensity ratio of the $^3P_1$-to-$^3P_0$ emission on pumping $^3P_1$ is shown in Fig. 4.

At the lowest temperatures, the fluorescent lifetime of $^3P_1$ is 2.81 ± 0.28 μsec, which is considerably different from the values of 4.5 and 4.8 μsec obtained by Low *et al.*[7] and by Barasch and Dieke,[6] respectively. By measuring the ratio of $^3P_0$-to-$^3P_1$ fluorescent intensities when exciting $^3P_1$, it was possible to determine the quantum efficiency of transfer of excitation from $^3P_1$ to $^3P_0$. A value of 29.7 μsec for τ_{rad} of $^3P_1$ was calculated by multiplying our measured value for the τ_{rad} of $^3P_0$ by the ratio of Dorman's[8] values for emission oscillator strengths of $^3P_1$ and $^3P_0$. By combining these numbers we calculate a value of 3.2 ± 0.4 μsec for the lifetime of the $^3P_1$-to-$^3P_0$ excitation transfer process. By comparison, if the 2.81-μsec fluorescent decay of $^3P_1$ is assumed to arise only from radiative decay to $^3H_5$ and nonradiative transfer to $^3P_0$, the transfer lifetime is 3.1 ± 0.3 μsec. Therefore, to within our accuracy of measurement, $^3P_1$ decays nonradiatively *only* to $^3P_0$ in the dilute crystal.

B. $PrCl_3$

The fluorescent lifetime of the $^3P_0$ state is plotted as a function of temperature in Fig. 2. Note that

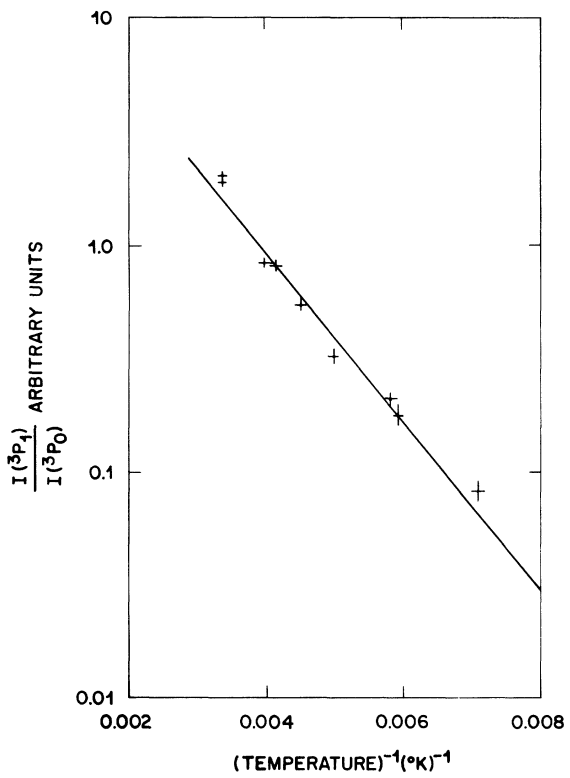

FIG. 4. Ratio of the fluorescence intensity of $^3P_1$ to that of $^3P_0$ as a function of temperature. The $^3P_0$ level is pumped in this experiment.

the lifetime at room temperature (370 nsec) is less than $\frac{1}{40}$ that of the dilute sample. Even at low temperatures the lifetime of $^3P_0$ in the concentrated crystal is still smaller than the dilute crystal by about a factor of $\frac{1}{4}$. The decay time is a monotonic function of temperature for the concentrated crystal as it was for the dilute case. These results are in almost total disagreement with Barasch and Dieke, who quote a room-temperature decay lifetime of ~12 μsec and a peculiar temperature variation.[11] In $PrCl_3$, *only the* $^3P_0$ *state fluoresces* and then only when the $^3P_0$ state is directly excited. This is in marked contrast to the situation in the dilute crystal where both the $^3P_0$ and $^3P_1$ states fluoresce when either is pumped. At low temperatures (<50 K) and sufficiently high-pumping flux ($\gtrsim 10^6$ W/cm^2), the threshold for stimulated emission was passed and the $^3P_1$ state emitted at 530 nm [$^3P_1(\mu=1) \rightarrow {}^3H_5(\mu=2)$].[10] However, no spontaneous fluorescence was ever observed from the $^3P_1$ state in $PrCl_3$. This behavior of the $^3P_1$ is consistent with the state being nonradiatively quenched in a time much less than the radiative lifetime of $^3P_1$. From Dorman's determination of the radiative lifetime in the dilute crystal and an estimate of the sensitivity of our detection system we deduce a nonradiative quenching time ≤ 1.5 nsec at low temperatures. It should be noted that the $^3P_1$ is *not relaxing to the* $^3P_0$ *state*, 590 cm^{-1} below it, since we do not see any of the characteristic emission from $^3P_0$ when pumping the $^3P_1$ state; nor is there any optical emission at wavelengths below 1 μm. The precise decay route for this process is still obscure but it almost certainly involves energy exchange with neighboring Pr ions.[15]

C. Rate Equations

In analyzing the time response of the $^3P_0$ and $^3P_1$ fluorescence decay we shall use an idealized three-level system which includes a single $^3P_1$ level, a $^3P_0$ level, and a single lower level which is a synthesis of all the low-lying states of Pr^{3+}. These states shall be designated by the subscripts 2, 1, and 0, respectively. Let n_1 and n_2 be the populations of $^3P_0$ and $^3P_1$, respectively; w_{21} is the nonradiative-decay rate for $^3P_1 - {}^3P_0$; and w_{12} is the inverse process and w_{10}, w_{20} are the decay rates from $^3P_0$ and $^3P_1$, respectively, to the lower level. We have the following rate equations for the evaluation of the population:

$$\begin{aligned} \dot{n}_1 &= -w_{10}n_1 + w_{21}n_2 - w_{12}n_1 \ , \\ \dot{n}_2 &= -w_{20}n_2 + w_{12}n_1 - w_{21}n_2 \ . \end{aligned} \tag{1}$$

Assuming a solution of the form

$$n_i = A_i^+ e^{\lambda_+ t} + A_i^- e^{\lambda_- t} \ ,$$

we obtain

$$2\lambda_\pm = -(w_{10}+w_{20}+w_{12}+w_{21}) \pm [(w_{10}+w_{12})^2 - (w_{20}+w_{21})^2 + 4w_{21}w_{12}]^{1/2} \ . \tag{2}$$

The pump pulse is much shorter than times involved in the emission so that we have essentially instantaneous excitation.

1. $^3P_0$ *Pumping*

For the case where $^3P_0$ is being pumped we have the initial condition ($t=0$)

$$A_1^+ + A_1^- = n \ , \quad A_2^+ + A_2^- = 0 \ , \tag{3}$$

where n is the number of excited atoms. The general solution may be written

$$n_1(t) = n\left[\left(1 - C\frac{w_{21}}{\lambda_- + w_{10} + w_{12}}\right)e^{\lambda_+ t} + C\frac{w_{21}}{\lambda_- + w_{10} + w_{12}}e^{\lambda_- t}\right] , \tag{4a}$$

$$n_2(t) = nC(e^{\lambda_+ t} - e^{\lambda_- t}) \ , \tag{4b}$$

$$C = \left(\frac{w_{12}w_{21} - (\lambda_+ + w_{20} + w_{21})(\lambda_- + w_{10} + w_{12})}{w_{12}(\lambda_- + w_{10} + w_{12})}\right)^{-1} \ . \tag{4c}$$

This expression may be simplified by substituting the detailed balance condition $w_{21}/w_{12} = \frac{1}{3}e^{\Delta/kt}$, where $\Delta = 591$ cm^{-1}. We can, therefore, use the fact that $w_{21} \gg w_{12}$ in our temperature regime. From the experimental data it is also true that $w_{21} \gg w_{10}$, w_{20}. We then have the approximate result

$$\lambda_+ \simeq -w_{10} \ , \quad \lambda_- \simeq (w_{20}+w_{21}) \ ,$$

$$n_1(t,T) = n(e^{-w_{10}t} + 3e^{-(w_{20}+w_{21})t - \Delta/kT}) \ , \tag{5a}$$

$$n_2(t,T) = 3ne^{-\Delta/kt}(e^{-w_{10}t} - e^{-(w_{20}+w_{21})t}) \ . \tag{5b}$$

We see that at 0 K, $^3P_0$ decays with a rate w_{10}. At high temperatures and at times such that $w_{21}t \gg 1$, the $^3P_1$ decay rate will be essentially the same rate as $^3P_0$, i.e., w_{10}. Note that we have *not* assumed that w_{10} and w_{20} are pure radiative decays so that they too may be temperature dependent.

The ratio of intensities of the decay from $^3P_1$ to that from $^3P_0$ is given by

$$R = \frac{\frac{1}{3}e^{\Delta/kT}e^{-w_{10}t} + e^{-(w_{20}+w_{21})t}}{e^{-w_{10}t} - e^{-(w_{20}+w_{21})t}} \ . \tag{6}$$

For times such that $t \gg w_{21}^{-1}$, this expression reduces to $R = e^{\Delta/kT}$. Figure 4 shows the fit of the experimental data to the above expression for R.

2. $^3P_1$ *Pumping*

The solution for this case is entirely analogous to the preceding one so we shall not duplicate any of the details. For this situation we have

$$n_1 = \frac{ne^{\Delta/kT}}{3 + e^{\Delta/kT}}(e^{-w_{10}t} - e^{-(w_{21}+w_{20})t}) \ , \tag{7a}$$

$$n_2 = \frac{n}{3+e^{\Delta/kT}}\left(3e^{-w_{10}t} + e^{\Delta/kT}e^{-(w_{21}+w_{20})t}\right) . \quad (7b)$$

At low temperatures, $n_2 = n\exp[-(w_{21}+w_{20})t]$ and the decay rate of $^3P_1$ is just $w_{21}+w_{20}$. This result was anticipated in Sec. III A when we determined the rate of transfer of excitation between $^3P_1$ and $^3P_0$. At room temperature, Eq. (7b) predicts a double exponential decay. The tail of this decay should have a time constant w_{10}^{-1} as we have indeed observed. (w_{10}^{-1} is the time constant of $^3P_0$ emission.) The apparent increase in the decay rate as temperature is decreased arises from the fact that the intensity of the slow decay (w_{10}) decreases with temperature until at sufficiently low temperatures only the fast decay is left.

IV. MULTIPHONON RELAXATION PROCESSES IN $^3P_1$, $^1I_6$ STATES

In Sec. III A we saw that the nonradiative relaxation time of the $^3P_1 \rightarrow {}^3P_0$ transition was ~3 μsec at low temperatures. The energy separation of these two manifolds is 591 cm^{-1} while the most energetic optical phonons[16,17] in $LaCl_3$ have energies below ~250 cm^{-1}. This relaxation process therefore requires at least three phonons to balance the energy. Although this relaxation decay is a third-order process, similar lifetimes for three-phonon decay[12] are observed for several other ions and host crystals.

We have also attempted to measure the nonradiative-decay time from $^3P_2$ to $^3P_1$. In our experiments we were never able to observe any emission from the $^3P_2$ state. There was, however, efficient energy transfer to the $^3P_1$ state when the $^3P_2$ was selectively excited. Within the resolution of our apparatus (20 nsec) we were unable to see any delay between the dye laser pulse and the onset of fluorescent emission from the $^3P_1$ level. A still smaller limit can be set from our earlier measurement of the start of stimulated emission from $^3P_1$ when pumping $^3P_2$.[4] We observed this delay to be less than 1.5 nsec (a detector with response time < 0.1 nsec was used in this measurement). We could also pump the $^1I_6$ states and, again, we observed no direct emission from $^1I_6$ and efficient transfer to $^3P_1$. The delay time was again ≤ 1.5 nsec. From Fig. 1 we see that $^3P_2$ is separated from $^3P_1$ by more than 1100 cm^{-1}. Therefore, direct relaxation to $^3P_1$ requires at least five phonons and a fifth-order process. The speed of this process is orders of magnitude faster than similar five-phonon processes reported in the literature.[12,13,18,19]

In view of this discrepancy, we have investigated the possibility that $^3P_2$ first relaxes to $^1I_6$ which in turn rapidly relaxes to $^3P_1$. The relaxation process postulated is shown in Fig. 5. Since the higher-energy levels of $^1I_6$ have not been observed reliably, we give our calculated values for these states. Note that in this process, the highest-order term is the three-phonon relaxation coupling $^3P_2$ and $^1I_6$. An immediate problem arises from the fact that there is a change in spin multiplicity[20] in the transition $^3P_2 \rightarrow {}^1I_6$ as well as in $^1I_6 \rightarrow {}^3P_1$. Since phonon interactions are not spin dependent, this process is forbidden in the pure Russell-Saunders (diagonal spin-orbit interaction) limit. However, in the intermediate-coupling limit, L and S are no longer "good" quantum numbers and states with the same J value may be coupled. In the general case, the state functions of interest are found to be[21]

$$|^3P_2)' = 0.959\,|^3P_2) + 0.281\,|^1D_2) - 0.029\,|^3F_2) , \quad (8a)$$

$$|^1I_6)' = 0.9985\,|^1I_6) + 0.0541\,|^3H_6) . \quad (8b)$$

Therefore, the transitions involving a change in spin are allowed although their magnitude is decreased in proportion to the size of the coefficients in Eqs. (8).

There has been a substantial quantity of recent theoretical and experimental work on the problem of multiphonon relaxation in solids and molecules.[22–25] Most of these have considered the strong electron-phonon coupling present in 3d element crystals or organic complexes. In the trivalent rare earths, the rather weak electron-phonon coupling allows a simpler approach utilizing

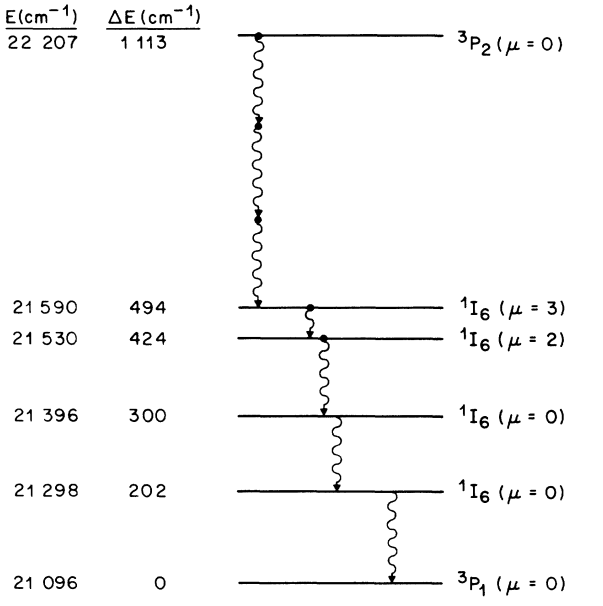

FIG. 5. Postulated decay path $^3P_2 \rightarrow {}^1I_6 \rightarrow {}^3P_1$. Each arrow indicates an emitted phonon. Arrows displaced horizontally indicate that the transitions are consecutive. The $^3P_2 \rightarrow {}^1I_6$ step is a three-phonon (simultaneous) transition.

the Born-Oppenheimer approximations and perturbation theory. The orbit-lattice interaction is then expressed as

$$H_{O\text{-}L} = \sum_i V(\vec{r}; Q_i) = V^0(\vec{r}) + \sum_i V_i(\vec{r})\, Q_i + \frac{1}{2} \sum_{i,j} V_{ij}(\vec{r})\, Q_i Q_j + \cdots \quad , \tag{9}$$

where V^0 is the static crystal potential energy, Q_i are normal modes of the crystal, and $V_i = \partial V^0/\partial Q_i$, $V_{ij} = \partial^2 V^0/\partial Q_i \partial Q_j, \ldots$. The relaxation phenomena are caused by the terms V_i, V_{ij}, while the basis functions of the electronic states are assumed to be diagonal in V^0. For the purpose of discussing multiphonon relaxation at low temperature and neglecting dispersion, Q_i is proportional to the creation operator (phonon number representation)

$$(n_i + 1 \,|\, Q_i \,|\, n_i) \sim (n_i + 1)^{1/2} \quad .$$

It is not our intention to attempt a detailed calculation of the relaxation rates involved in the $LaCl_3$: Pr system. We shall be content to discuss relative magnitudes and qualitative features of the process. We will therefore only use the lowest-order term in the phonon operators in Eq. (9), $V_i Q_i$. The p-phonon transition rate may be written

$$W^{(p)} = \frac{2\pi}{\hbar} \sum_{\substack{\text{lattice} \\ \text{vectors}}} |(n_p + 1 \,|\, Q_p \,|\, n_p) \cdots (n_i + 1 \,|\, Q_1 \,|\, n_1)|^2 \times \sum_{\substack{\text{intermediate} \\ \text{states}}} \left| \frac{(\psi_B \,|\, V_p \,|\, \psi_{p-1}) \cdots (\psi_1 \,|\, V_1 \,|\, \psi_A)}{(E_{p-1} - E_A + \hbar\omega_{p-1} + \cdots + \hbar\omega_1) \cdots (E_i - E_A + \hbar\omega_i)} \right|^2 \delta(E_B - E_A + \hbar\omega_p + \cdots + \hbar\omega_1) \quad . \tag{10}$$

This expression is still intractible when one considers that we must still sum over the density of states of the vibrational modes and over the intermediate electronic states. The main physical content of this expression can be elucidated by writing the result in the following form:

$$W^{(p)} = \frac{2\pi}{\hbar^2} \times \left| \frac{(\psi_B \,|\, \langle q \rangle_{av} V_p \,|\, \psi_{p-1}) \cdots (\psi_1 \,|\, \langle q \rangle_{av} V_1 \,|\, \psi_A)}{\langle \Delta E \rangle_{av}^{p-1}} \right|^2 g(\omega) \quad , \tag{11}$$

where $\langle \Delta E \rangle_{av}$ is the average energy denominator, $g(\omega)$ is an appropriate joint density, and $\langle q \rangle_{av}$ is an average amplitude for the vibrational modes.

The most important optical modes for the multiphonon case will be the most energetic ones,[26] those with energies of ≈ 200 cm^{-1}.

For a single-phonon relaxation, Eq. (11) reduces to

$$W^{(1)} = \frac{2\pi}{\hbar^2} \left| (\psi_B \,|\, \langle q \rangle_{av} V_1 \,|\, \psi_A) \right|^2 g(\omega) \quad . \tag{12}$$

The average amplitude is approximately given by

$$\langle q^2 \rangle_{av}(\text{optical}) \cong \frac{\hbar}{2M\omega} \frac{1}{1 - e^{-\hbar\omega/kT}} \quad , \tag{13a}$$

$$\langle q^2 \rangle_{av}(\text{acoustic}) \cong \frac{\hbar\omega}{2M\omega_D^2} \frac{1}{1 - e^{-\hbar\omega/kT}} \quad , \tag{13b}$$

where M is the reduced mass and ω_D is the Debye frequency. The magnitude of $V_p \simeq \partial V^0/\partial Q_p$ may be written

$$|V_p| \approx c\,|V^0|/a \quad , \tag{14}$$

where a is the nearest-neighbor distance (≈ 3 Å in $LaCl_3$) and c is a constant which depends on the order of the spherical harmonic and the particular mode. Typical values for c range between 1 and 20 (see Ref. 27 and 28). For optical modes we get $\langle q \rangle_{av}/a \sim 10^{-2}$–$10^{-3}$, $cV^0 \sim 10^{-2}$–10^{-4} cm^{-1}, and $g(\omega) \sim 10^{-9}$–10^{-10} sec. The matrix elements of the angular parts of V_p, i.e., $(\psi_B \,|\, C_K^Q(\theta, \phi) \,|\, \psi_A)$, where $C_K^Q(\theta, \phi)$ is a spherical harmonic, typically range between 0.01 and 1 (when the matrix element is not identically zero due to selection rules). If we substitute the maximum estimates above into Eq. (12) we see that the single-optical-phonon transition rate can be as large as 10^{16} sec^{-1}. Hence, single-phonon transition rates of the order of 10^{13} sec^{-1} would not be unreasonable in many cases. It is not surprising therefore that rapid transition rates occur in some cases for the three-phonon case, provided the interaction term $\langle q \rangle_{av} (\psi_l \,|\, V_l \,|\, \psi_{l-1})$ is not too small relative to the average energy denominator $\langle \Delta E \rangle_{av}$.

Specializing Eq. (11) to the $^3P_2 \rightarrow {}^1I_6$ relaxation case, we get

$$W^{(3)}(^3P_2 \rightarrow {}^1I_6) = \frac{2\pi g(\omega)}{\hbar^2} \left| \frac{(^1I_6 \,|\, \langle q \rangle_{av} V_3 \,|\, ^1I_6)(^1I_6 \,|\, \langle q \rangle_{av} V_2 \,|\, ^1I_6)(^1I_6 \,|\, \langle q \rangle_{av} V_1 \,|\, ^3P_2)}{\langle \Delta E \rangle_{av}^2} \right|^2 \quad . \tag{15}$$

Taking account of the intermediate coupling corrections in (8) and substituting for $\langle \Delta E \rangle_{av} \simeq 280\ \mathrm{cm}^{-1} \simeq 280 \times 2 \times 10^{-16}$ erg,

$$W^{(3)} = \frac{2\pi g(\omega)}{\hbar^2} (0.28)^2 \left| \frac{(^1I_6|\langle q \rangle_{av} V_3 |^1I_6)(^1I_6|\langle q \rangle_{av} V_2 |^1I_6)(^1I_6|\langle q \rangle_{av} V_1 |^1D_2)}{(5.6)^2 \times 10^{-28}} \right|^2 . \quad (16)$$

The uncertainty in this (and most other) calculations make detailed evaluation of Eq. (16) rather futile. What we primarily wish to point out is that, by their nature, the matrix elements connecting $^1I_6$ states in Pr^{3+} are exceptionally large for rare-earth ions. This is partly reflected in the fact that the upper $^1I_6$ states are so broad that they are undetectible in absorption. Calculation of the functions $(^1I_6, \mu | C_2^q | {}^1I_6, \mu)$ show that the largest such matrix elements are greater than unity, about a factor of between 3 and 30 times greater than that typical of rare-earth ions. In particular, they are substantially greater than the values occurring in the cases considered by Riseberg and Moos[12,18] who studied several cases of three-phonon relaxation in rare earths. This fact is not only sufficient to overcome the reduction due to the intermediate-coupling coefficient $(0.28)^2 \simeq 0.08$ but to allow a relaxation time several orders of magnitude greater than the "typical" values given in the curves in Refs. 12 and 18.

The consecutive portions of the decay illustrated in Fig. 5 (single-phonon decays) may be safely assumed to be instantaneous within the time scale we are considering since we saw that single-optical-phonon relaxation will typically[29] take place in $\sim 10^{-13}$ sec. Even the intermediate-coupling factor $(0.054)^2 \simeq 0.003$ necessary for the final step $^1I_6(^3H_6) \rightarrow {}^3P_1$ will not be a bottleneck for this case.

The $^3P_1$ state relaxes to $^3P_0$ by a three-phonon process in about 3 μsec, *at least* 2000 times more slowly than the $^3P_2 \rightarrow {}^3P_1$ relaxation. There are two reasons for this large difference in relaxation rates; one is the size of the matrix elements which we discussed above. The second reason involves the fact that for a potential term $C_K^Q(\theta, \phi)$ to have a nonzero matrix element between states $|LSJ>$ and $|LSJ'>$, we must have $K \leq J + J'$ (this is one-half of the triangle rule for adding angular momentum). For a transition $^3P_1 \rightarrow {}^3P_0$, $J + J' = 1$. However, these states both have the same parity (to first order in the odd crystal field) so that an odd potential term $C_1^q(\theta, \phi)$ cannot couple them while the even term $C_2^Q(\theta, \phi)$ also gives zero coupling because the triangle rule is violated. This restriction may be lifted by taking into account J mixing by the static crystal field V^0, i.e.,

$$(^3P_2 | V^0 | {}^3P_{1,0}) / \delta E$$

(see reference cited in Ref. 19). However, for higher-order phonon processes it is not necessary to rely on static mixing. The three-phonon process can be described as follows:

$$W^{(3)} = \frac{2\pi}{\hbar^2} g(\omega) \left| \frac{(^3P_0|\langle q \rangle_{av} V_3 |^3P_2)(^3P_2|\langle q \rangle_{av} V_2 |^3P_1)(^3P_1|\langle q \rangle_{av} V_1 |^3P_1)}{\langle \Delta E \rangle_{av}^2} \right|^2 . \quad (17)$$

Note that $^3P_2$ appears as a virtual intermediate state. This fact results in a larger energy denominator since $^3P_2$ is $\sim 1700\ \mathrm{cm}^{-1}$ above $^3P_0$. The result is that $\langle \Delta E \rangle_{av} \sim 750\ \mathrm{cm}^{-1}$ in this case compared to the 280 cm^{-1} we would have for $\langle \Delta E \rangle_{av}$ if no new intermediate state were required; $(280/750)^4 \simeq 0.02$. This reduction is far less than that introduced by the static mixing described above.

The largest matrix elements of C_2^Q within ^3P states are about 0.3. Taking into account the ratio of matrix elements and average energy denominators *and* the intermediate coupling required for $^3P_2 \rightarrow {}^1I_6$ we expect

$$W^{(3)}(^3P_2 \rightarrow {}^1I_6) \approx 5500 W^{(3)}(^3P_1 \rightarrow {}^3P_0) . \quad (18a)$$

The experiments show that

$$W^{(3)}(^3P_2 \rightarrow {}^1I_6) \geq 2000 W^{(3)}(^3P_1 \rightarrow {}^3P_0) . \quad (18b)$$

The point of these calculations has been to demonstrate that the exact nature of the relaxing states cannot be ignored in estimating multiphonon relaxation time. The general curves in Refs. 12 and 18 are, indeed, very useful but we have seen that a special case can fall three orders of magnitude outside of this pattern.

ACKNOWLEDGMENT

The authors are indebted to H. R. Guggenheim who supplied the crystals used in these experiments.

[1] *Handbook of Lasers*, edited by Robert J. Pressley (The Chemical Rubber Co., Cleveland, Ohio, 1971), pp. 350.

[2] D. P. Devor, B. H. Soffer, and M. Robinson, Appl. Phys. Lett. 18, 122 (1971).).

[3]F. Varsanyi, Appl. Phys. Lett. **19,** 169 (1971).
[4]K. German, A. Kiel, and H. Guggenheim, Appl. Phys. Lett. **22,** 87 (1973).
[5]H. Weber, T. C. Damen, H. G. Danielmeyer, and B. C. Tofield, Appl. Phys. Lett. 22, 534 (1973).
[6]G. Barasch and G. H. Dieke, J. Chem. Phys. **43,** 988 (1965).
[7]W. Low, J. Makovsky, and S. Yatsiv, in *Quantum Electronics III,* edited by P. Grivet and N. Bloembergen (Columbia U. P., New York, 1964), pp. 655-671. Using x-ray excitation, Low *et al.* seem capable of observing a number of fluorescence lines which have never been seen under optical pumping. Since different mechanisms may be involved (including crystal damage), some caution should be observed in comparing their results to the present work and those of Refs. 6 and 8.
[8]E. Dorman, J. Chem. Phys. **44,** 2910 (1966).
[9]In this paper, the fluorescent decay rate/time refers to the sum of all the radiative-decay paths and all nonradiative-decay paths. In other words, the fluorescent decay rate is the inverse of the observed fluorescent lifetime of a particular level.
[10]The fluorescence lines used in this experiment were either the 645-nm $^3P_0 \rightarrow {}^3F_2$ ($\mu = 2$) or the 619-nm $^3P_0 \rightarrow {}^3H_6$ ($\mu = 2$) emission lines. The crystal quantum number μ and complete energy-level scheme are given by Gerhard Dieke, in *Spectra and Energy Levels of Rare Earth Ions In Crystal* (Interscience, New York, 1968), pp. 116 and 196-199.
[11]In the case of the $^3P_0$ emission in $LaCl_3$:1-at.% Pr, Barasch and Dieke (Ref. 6) claim that the decay time peaks at a temperature $\approx$ 77 K (τ = 16.7 μsec) with τ(4.2 K) = 13.4 μsec and τ(300 K) = 10.2 μsec.
[12]L. A. Riseberg and H. W. Moos, Phys. Rev. **174,** 429 (1968).
[13]M. J. Weber, Phys. Rev. **171,** 283 (1968); J. Chem. Phys. **48,** 4774 (1968).
[14]On the time scale of these experiments, decay rates of less than 10^3 sec^{-1} are essentially negligible.
[15]For example, an ion initially in the $^3P_1$ ($\mu = 1$) state may relax to $^1D_2$ ($\mu = 0$), while a neighboring ion initially in the ground state [$^3H_4$ ($\mu = 2$)] is excited to the $^3H_6$ ($\mu = 2'$) state: $^3P_1$ ($\mu = 1$) + $^3H_4$ ($\mu = 2$) $\rightarrow {}^1D_2$ ($\mu = 0$) + $^3H_6$ ($\mu = 2'$) + 3 cm^{-1}. Energy migration can be very rapid when the activation energy is as small as 3 cm^{-1} [W. B. Gandrud and H. W. Moos, J. Chem. Phys. **49,** 2170 (1968); L. G. Van Uitert, J. Electrochem. Soc. **114,** 1048 (1967).
[16]F. T. Hougen and S. Singh, Proc. R. Soc. A **227,** 193 (1964).
[17]Using the data of Ref. 16 and some results in T. C. Damen, A. Kiel, S. P. S. Porto, and S. Singh, Solid State Commun. **6,** 671 (1968), the symmetry designations (C_{6h} symmetry) and energies of the optical phonons at k = 0 are E_{2g} (108 cm^{-1}), A_g (179 cm^{-1}), E_{2g} (179 cm^{-1}), E_{1g} (186 cm^{-1}), E_{2g}(210 cm^{-1}) and E_{2g} (217 cm^{-1}). There are two B_{2g} "silent" modes whose energies are estimated to be about 85 and 250 cm^{-1}, [See P. Dawson and G. Schaak, J. Phys. Chem. Solids (to be published)].
[18]H. W. Moos, J. Lumin. **1,** 106 (1970).
[19]The relaxation time for the five-phonon process discussed here was calculated by A. Kiel, in *Quantum Electronics*, edited by P. Grivet (Columbia U. P., New York, 1964), Vol. 1, p. 765. The time constant for this case was determined as $\tau \simeq 100$ μsec.
[20]The change in spin together with the fact that the upper state of $^1I_6$ were unknown (it was not realized that the over-all splitting of $^1I_6$ could be as large as the 400 cm^{-1} calculated here) are the reasons that this process was not considered previously in Ref. 19.
[21]M. J. Weber, J. Chem. Phys. **48,** 4774 (1968).
[22]M. D. Sturge, Phys. Rev. B 8, 6 (1973).
[23]Baruch Barnet and Robert Englman, J. Lumin. **3,** 37 (1970).
[24]Abraham Nitzan and Joshua Jortner, J. Phys. A **56,** 2079 (1972).
[25]S. J. Lin, J. Chem. Phys. **56,** 2648 (1972).
[26]In Ref. 22, Sturge points out that due to details in the density of states, the most energetic modes need not be the most important (i.e., $W^{(p+n)} > W^{(p)}$). However, for rare earths, and particularly rare earths in $LaCl_3$, all evidence seems to indicate that a *minimum number of modes* always dominates the relaxation. See Refs. 12 and 18.
[27]Z. Sroubek, M. Tachiki, P. H. Zimmerman, and R. Orbach, Phys. Rev. **165,** 435 (1968).
[28]A. Kiel, in *Paramagnetic Resonance* edited by W. Low (Academic, New York, 1963), p. 525.
[29]One or more of the "consecutive" transitions within the $^1I_6$ manifold will involve emission of an acoustic phonon. In this case Eq. (13b) is used for $\langle q^2 \rangle_{av}$ with $\omega_D \approx 100$ cm^{-1}. The $g(\omega)$ in Eq. (12) is replaced by the density of states $\rho(\omega) = N\omega^2/\omega_D^3$, where N is the number of ions/cm^3. For $\hbar\omega$ greater than 50 cm^{-1}, the relaxation time for transitions within $^1I_6$ would be expected to occur in times less than 10^{-10} sec (see Ref. 28 for several similar examples). The exceedingly large linewidths of the $^1I_6$ states confirm our estimates of very rapid relaxation.